AIAA Propulsion and Energy Forum
10-12 July 2017, Atlanta, GA
53rd AIAA/SAE/ASEE Joint Propulsion Conference

Role of Pressure and Aluminum Size in Solid Propellant CCP Generation

Filippo Maggi*, Stefano Dossi†, Christian Paravan‡, Stefania Carlotti§, Luciano Galfetti¶
Politecnico di Milano, Milan, MI, 20156, Italy

Aluminum combustion in solid propellants generates condensed products leaving the burning surface. The population of this particles is quite wide, spanning from smoke-oxide to molten metal drops. Their properties depend upon both intrinsic propellant features and combustion conditions (e.g. composition, microstructure, combustion pressure, and propellant burning rate). In propellants, aluminum is typically used in the shape of a micrometric powder. This class of energetic materials produces spherical agglomerates having the size between some tens to few hundreds of micrometers. When the metal fuel turns to nanometric, flake-kind aggregates emerge from the burning surface. Some macroscopic properties, such as the burning rate, are affected. This paper presents some results obtained from a set of aluminized propellants based on inert binder (hydroxyl-terminated polybutadiene) and ammonium perchlorate. The effect of both powder size and pressure is explored in terms of ballistics and condensed combustion residues. A non-straightforward trend with pressure emerges when the condensed combustion products of propellants containing micro-aluminum and nano-aluminum are compared.

Nomenclature

μAl05	micrometric aluminum, nominal size 5 µm
μAl30	micrometric aluminum, nominal size 30 µm
AP	ammonium perchlorate
CCP	condensed combustion products
DTA	differential thermal analysis
EEW	electric explosion of wire
HTPB	hydroxyl-terminated polybutadiene
nAl	nanometric aluminum
nAl100L	nanometric aluminum, coated with stearic acid, nominal size 0.1 µm
nAl800	sub-micrometric aluminum, nominal size 0.8 µm
SSA	specific surface area
TGA	thermogravimetric analysis
TMD	theoretical maximum density

Symbols

ρ_p	propellant density
d	diameter
D_{43}	mass-mean particle size
m	exponent in particle burning time relation
p	pressure
r_b	burning rate
t_b	burning time

I. Introduction

Aluminum powder represents an interesting fuel for solid rocket propellants. This metal is commonly adopted in civil applications since it leads to the improvement of both density and gravimetric specific impulse.[1] In its micrometric form the powder is relatively cheap, available on a large scale, and features a low level of toxicity.[2] Aluminum particles tend to agglomerate at the burning surface. In connection to this behavior, two-phase flow behavior, incomplete combustion, and contribution to nozzle throat erosion represent some aspects that were addressed in the competent literature across the years. Both experimental

*Assistant Professor, Dept. Aerospace Science and Technology, Via La Masa 34, AIAA Senior Member
†Post-doctoral Research Fellow, Dept. Aerospace Science and Technology, Via La Masa 34
‡Adjunct Professor, Dept. Aerospace Science and Technology, Via La Masa 34, AIAA Member
§PhD Student, Dept. Aerospace Science and Technology, Via La Masa 34
¶Full Professor, Dept. Aerospace Science and Technology, Via La Masa 34, AIAA Senior Member

and modeling approaches were used with the aim of understanding and quantifying the penalties to the delivered performance.[3–8] In this respect, an AGARD publication by Reydellet reported an estimation of about 3 % specific impulse decrement due to two-phase flow, on the basis of experimental data.[9] A NASA publication reported a loss estimation of up to 5 %, having a common value between 1.5 and 2.5 %.[10]

Collection techniques (mainly impactors[11] or quench bombs[12]) as well as visualization methods[13] have been employed to investigate the variation of CCP size as a function of both propellant formulations and combustion environment parameters. Images from compositions containing micrometric powders show the evolution of metal aggregates into spherical metal drops. Once the pressure is incremented, smaller fragments leaving the burning surface can be observed (pocket and sub-pocket agglomeration). On the contrary, if slow-burning combustion processes are present, metal drops move along the inter-pocket bridges on the surface and merge with other metal formations (inter-pocket agglomeration).[12] For similar compositions, collected combustion product size decrements with pressure and is influenced by the heterogeneous nature of the propellant.[12,14] When nanometric powders are employed, a completely different mechanism is observed, showing flake-kind structures leaving the burning surface. The size of these structures is rather difficult to be analyzed with a video technique, for two specific reasons. First, the enhanced burning rate increments the release of the metal flakes and their departing velocity, making their observation more difficult at high magnification. Second, the porous flake-kind structure prevents from a proper quantification of particle mass and size. In this specific subject, consistent data from CCP collection are not common in the competent literature and, in particular, a parametric study that crosses the effect of metal size and combustion pressure is missing at authors' knowledge. The present work summarizes some experimental results obtained from the analysis of different solid propellant compositions containing aluminum powder of decreasing size, burning under multiple pressure conditions. Data sets presented in this paper refer to ballistic behavior of the tested energetic materials and particle size distribution of the generated agglomerates.

II. Background

The reduction of aluminum size in one propellant composition does not modify the energy content of the material, unless the size of the particles become too small. In this latter case, the oxide contained in the metal fuel may become significant.[15] From a ballistic performance viewpoint, the introduction of micrometric aluminum in AP-based propellants does not produce sensible improvements, as reported by Steinz and co-authors in Ref.[16] More recent works have underlined that such consideration is correct till the metal particle size is above a certain micrometric level. Experimental data available in the literature have demonstrated that the progressive reduction of the metal particle size increments the reactivity of the energetic material.[17] Specifically for the composite propellants, an enhancement of the burning rate was observed.[18]

The use of nanoaluminum in propellants and in energetic materials has been considered since more than a decade. Its use in solid propellants has been proposed by a long list of authors. Only a very short selection is reported hereafter. Ivanov and Tepper considered the use of nanoaluminum in propellants about two decades ago.[19] Measurement of ballistic properties and qualitative observations of the burning surface were initially performed by Dokhan and Price on propellants containing mixed nano-micrometric aluminum and a blend of fine-coarse oxidizer.[20] Analyses of condensed combustion products generated by nano-structured propellants were developed by Babuk *et al.*[21] and Glotov and co-authors.[22] In the recent years several reviews have been made available, either generalized or focused on some peculiar aspects of nanoaluminum combustion. Dreizin *et al.* and Yetter *et al.* produced journal papers about nano-metal use, focusing on nanoaluminum for some peculiar combustion and production aspects.[23,24] The SPLab-POLIMI research group has been very active in the field of nanoaluminum analysis. Pre-to-post burning analyses of nanoaluminum in AP-based propellants were presented by Galfetti *et al.*[25–27] and DeLuca *et al.*[28–30] A global overview of these research activities were recently summarized by DeLuca *et al.*[31,32] and Paravan *et al.*[15]

The structure of the agglomerates leaving the burning surface of propellants loaded with micrometric aluminum has been described by Price.[33] A clear imaging sequence of the process at low pressure was reported in more recent papers.[27,34] The metal drops lifting from the surface are generated through an aggregation-to-agglomeration process which was precisely addressed in a paper by DeLuca and co-authors.[18] In the same paper, the authors also noted that the burning rate behavior and agglomeration attitude changed as the size of aluminum was reduced from micrometric to nanometric. In an earlier paper, Galfetti *et al.* disclosed several interesting properties of nanoaluminum-based propellant combustion.[27] Specifically, the

burning rate was observed to increase of up to about 100 %, in the case of inert binder. Moreover, particles leaving the surface featured a flake-like shape (see Fig. 1). It was not possible to observe directly if the flakes eventually collapse into a drop as do the aggregates generated by micrometric aluminum powders, but the collected materials result in a quite spherical shape.[25] In any case, the structures observed in the video recordings once they leave the propellant surface seemed to be porous, fine, and generated by a set of partially molten particles, probably sintered. The paper also highlighted that the crystalline phases found in CCP released from propellants containing aluminum in nanometric and micrometric shape were different and the features were pressure-dependent. Other authors confirmed that the pressure plays a fundamental role in ruling the agglomeration since it controls the burning rate. As an example, Babuk and co-authors reported several tests where the CCP size was decreased as the pressure was incremented.[12] Bandera *et al.* and Maggi *et al.* found some pressure correlation with the size of agglomerates, connected to the pocket structure.[14,35]

Figure 1. CCP leaving the burning surface of a nAl-based propellant (courtesy of Galfetti *et al.*[27])

The incremented burning rate of propellants with nanoaluminum is a consequence of an increased heat feedback from the flame back to the combustion surface. In order to have enthalpy release from a combustion process, the fuel must be capable of igniting and should have time to react with the oxidizer. Short combustion time may result in incomplete oxidation. About ignition, Pokhil reported that micrometric aluminum in air starts reacting at the melting point of the alumina. However, this value is very sensitive to the atmosphere where the process is occurring. In the flow of propellant combustion products such value can be much lower.[36] The high ignition temperature of micrometric aluminum powders is also confirmed by different experimental tests. In data reported by Paravan *et al.* such class of metal fuel ignites above the limits of the experimental rig at fast heating rate, say above 1800 K.[15] The increment of the specific surface of the powder causes earlier ignition and faster release of the oxidation enthalpy. The anticipation of the powder ignition onset was widely investigated with different techniques, under both slow and fast heating rate conditions. Nanoaluminum can ignite as low as about 800 K to 900 K in air under thermogravimetric test conditions. This value is further decremented of about 100 K for faster temperature ramps, more similar to propellant-kind conditions.[37] The burning time of aluminum particles was widely investigated, in association to the diffusive-to-kinetic transition of the combustion regime. The dependence on the size is quite evident from experimental data reported by Huang and co-authors.[38] The transition between the diffusion-limited combustion regime to the kinetic-dominated oxidation occurs in the range around 10 µm. In both cases the combustion time can be reduced by a power-law fitting in the shape $t_b = d^m$. Different positive exponents are identified according to the regime ($m = 1.8$ for the diffusive regime and $m = 0.3$ in the kinetic regime) but the decrement of the size always leads to shorter burning times. At the same time, a reduction of the metal content can be observed when the powder becomes smaller, being the aluminum naturally covered by an oxide layer which thickness does not scale.[23] It follows that the enthalpy release will occur faster for smaller particles but the total available energy budget of the reaction decreases. As a possible indication of prompt metal ignition, high speed videos documenting the flake-kind combustion process of nanoaluminum showed brighter aspect compared to spherical agglomerates emerging from propellants containing micrometric aluminum.[20,27]

III. Experimental

A. Propellant compositions

A series of four AP/Al/HTPB propellant formulations have been produced. Every batch featured the same nominal composition (respectively, 68 wt.%/18 wt.%/14 wt.%). For the oxidizer, a bimodal blend of 200 µm coarse and ball-milled fine particles was used. Four different Aluminum fuel powders were considered.

- μAl30: Spherical propulsion-grade powder having the nominal size of 30 µm.
- μAl05: Spherical propulsion-grade powder having the nominal size of 5 µm.
- nAl800: Sub-micrometric powder by US Research Nanomaterials Inc. (USA) with nominal size of 0.8 µm.
- nAl100L: Nanometric powder (produced using EEW) by Advanced Powder Technologies LLC (Russia) with nominal size of 0.1 µm, coated with stearic acid.

The propellants have been cured with isocyanates using a tin-based catalyst and did not include any ballistic modifier. The details of the compositions along with the measured density (via buoyancy technique) are given in Table 1.

Id.	AP	HTPB	μAl30	μAl05	nAl800	nAl100L	ρ_p, g cm^{-3}
P-μAl30	68	14	18	-	-	-	1.749 ± 0.010
P-μAl05	68	14	-	18	-	-	1.756 ± 0.004
P-nAl800	68	14	-	-	18	-	1.754 ± 0.011
P-nAl100L	68	14	-	-	-	18	1.744 ± 0.017

Table 1. Compositions of tested propellants in weight percent and measured density. The oxidizer is made by 58 parts of coarse AP with 200 µm nominal size and 10 parts of ground AP (finer than 20 µm). The TMD is 1.761 g cm^{-3}

B. Metal fuel ingredients

A preliminary pre-burning characterization of the metal fuel ingredients allowed a comparison between physical and reactivity properties of the different powders. The following data have been processed.

- Mass-mean particle size D_{43} was obtained using laser diffraction technique (unless differently stated, dry dispersion was used).
- Specific surface areas (SSA) were derived from adsorption isotherm analysis and Brunauer-Emmett-Teller method.[39]
- The active metal content was evaluated using aluminum hydrolysis method.[40]
- Low heating rate reactivity in air was assessed using a simultaneous DTA/TGA running with a purging flow of 150 mL min^{-1} and a temperature ramp of 10 K min^{-1}.

The information on particle size, SSA, and metal content are reported in Table 2 while DTA/TGA signals are plotted in Fig. 2 and Fig. 3.

The expected trends are verified as the reduction of the powder size leads to a decrement of the active metal content and an increment of the specific surface area. In addition, a reduction of the diameter leads to an increment of the reactivity. This latter aspect can be observed by the analysis of both the mass increment of the TGA and the differential temperature of the DTA. If the single curves are compared, it is interesting to see that the coarsest aluminum μAl30 does not produce an evident exothermic peak prior to the melting point of the metal, clearly indicated by the endothermic peak at 660 °C. The peak is present in all other curves. Only the nAl100L shows only a limited sign of melting. For this specific material, a consistent fraction of the metal may be depleted during the first oxidation peak, as indicated by the mass increment

Table 2. Properties of tested powders

	μAl30	μAl05	800nm	100nm
D_{43}, µm	49.7	5.1	1.7	0.14 (wet)
Specific surface area, $\mathrm{m\,g^{-1}}$	0.1	1.2	3.6	10.5
Active Al content	99.6 ± 0.1	95.9 ± 0.7	87.4 ± 0.2	89.4 ± 1.1

of the TGA. The nAl800 and the μAl05 perform in a similar manner from a calorimetric viewpoint. They both present a limited exothermic peak at about 600 °C. Then the melting is evident. This is probably due to similitude of the effective powder size. The nAl800 and nAl100L do not have similar calorimetric traces. The effective size of the ingredients is too different and the reactivity is influenced. Despite these samples have different temperature vs. mass behavior, they present similar final mass gain. The nAl100L takes more mass at the lower temperatures while the nAl800 requires a hotter environment.

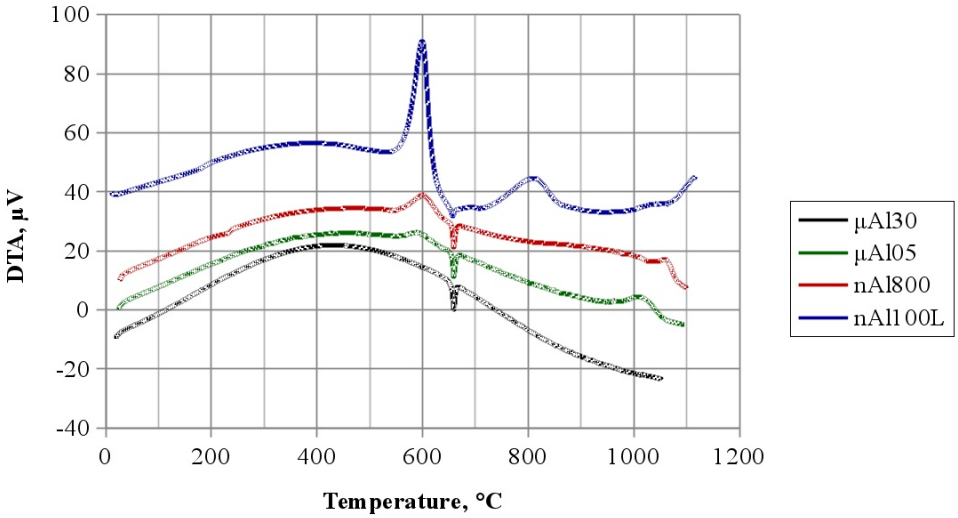

Figure 2. DTA traces of metal powders tested in air (Exo-up convention). Purging flow $150\,\mathrm{mL\,min^{-1}}$**. Temperature ramp** $10\,\mathrm{K\,min^{-1}}$**. Curves are shifted for better comparison.**

C. Experimental rigs for combustion characterization

1. Burning rate analysis

The experimental ballistic characterization was performed in a stainless steel strand burner of 2-liter volume and equipped with optical accesses for propellant combustion video recording. Burning tests were executed at different pressures between 5 and 40 bar in nitrogen atmosphere. The pressure was kept constant by a set of electrovalves controlled through an analog regulator and an external gauge. A commanded hot wire triggered the ignition. A video camera linked to a personal computer recorded the propellant combustion. The burning rate of the sample was derived from the digital post-processing of the video recording, after proper pixel-size calibration. At least three valid experiments have been run for each combustion condition. A representation of the experimental assembly is reported in Fig. 4(a). The propellants were cut in samples of 4x4x30 mm and side-inhibited by a solution of low molecular weight polymer to guarantee a flat flame front.

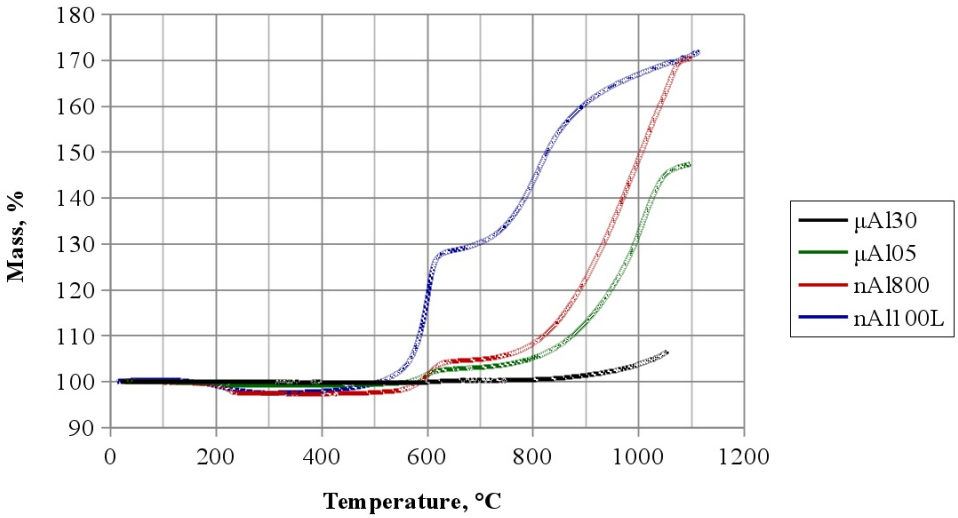

Figure 3. TGA traces of metal powders tested in air. Purging flow $150\,\mathrm{mL\,min^{-1}}$**. Temperature ramp** $10\,\mathrm{K\,min^{-1}}$**.**

2. CCP collection quench bomb

The combustion chamber used for the CCP collection consisted of a windowless stainless steel vessel of 1.4-liter volume. The sample was burnt in an upside-down configuration. Beneath the burning sample, a quenching pool collected the solid particles ejected from the propellant strand. A halogen-based hydrocarbon was used to quench the particles few millimeters far from the burning surface. The pressure control system was similar to the one described for the burning rate setup. Also in this case, the vessel was pressurized with nitrogen gas. Tests were run at 10 and 40 bar. After the collection, particles were treated and measured with a laser granulometer to obtain a particle size distribution. Three tests have been performed per each condition. A representation of the experimental rig is shown in Fig. 4(b). For this kind of test, a 8x8x30 mm side-inhibited sample was used.

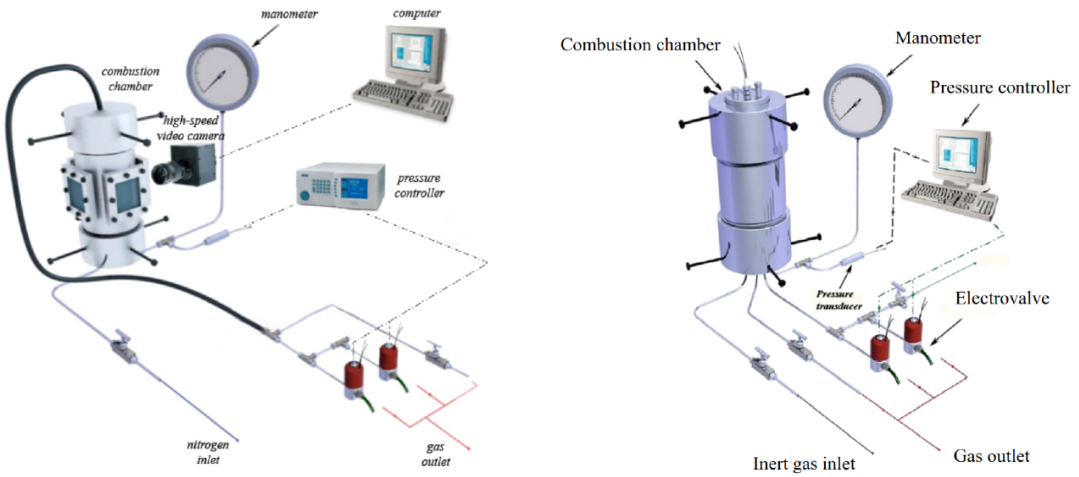

(a) Experimental rig for ballistic characterization

(b) Collection chamber for characterization of CCP

Figure 4. Experimental rigs used for the characterization of propellant combustion properties

IV. Results and discussion

A. Ballistic properties

The burning rate results and the corresponding Vieille's law data are reported in Fig. 5. As expected, the progressive reduction of the metal size causes a higher burning rate. From the micrometric baseline to the smallest nanometric aluminum tested in this work the burning rate gains about 100% at the highest tested pressure. The P-nAl100L obtains also the highest pressure exponent. This material has evidenced the smallest particle size, associated with the more vigorous oxidation peak before metal melting under slow heating rate tests. In this scenario, the lowest metal content does not appear to have much importance. The behavior of the P-nAl800 is almost overlapped with the ballistic properties of the μAl05 and features the lowest pressure exponent among the tested materials. The similarity between P-nAl800 and μAl05 may be traced back to the powder properties. Despite the nAl800 is finer, the difference does not suffice to grant distinctive ignition and oxidation capabilities of the particles at the burning surface level. The results from the slow heating rate tests can partially support this consideration, having in mind that the temperature gradients are some order of magnitude higher in propellant combustion. Finally, the P-μAl30 demonstrates the lowest burning rate across the entire tested range. The μAl30 powder was already identified in Section B as the less reactive material due to its coarser size and consequent smaller SSA.

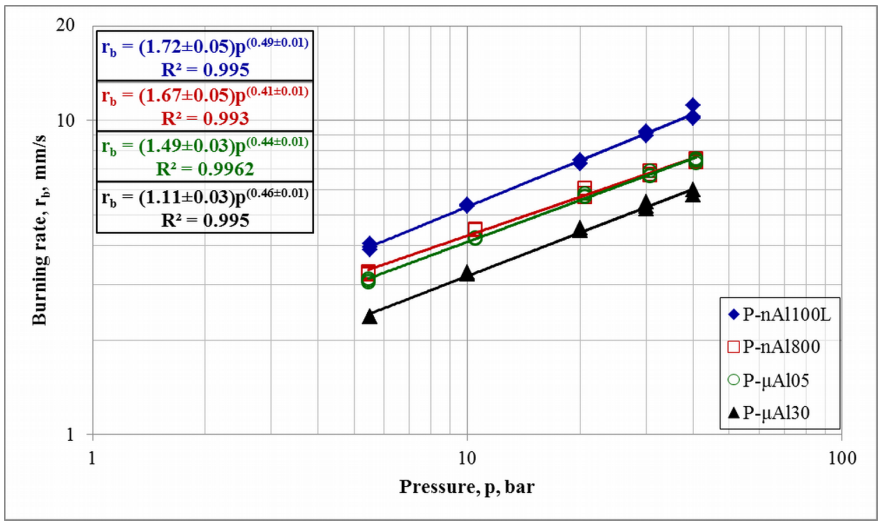

Figure 5. Burning rate characterization

B. Condensed combustion products

The results obtained from the quench-bomb collector are reported hereafter. In Fig. 6 the values of the mass-mean diameter D_{43} of collected residues and the confidence interval of the measures are represented. The error estimation was computed using a t-student distribution on a set of three experiments and a confidence level of 95 %. In this respect, the wide interval associated to the CCP size of the P-nAl800 propellant should be attributed to the presence of hard clusters in the raw powder. Such fragments were observed to lift off from the burning surface during the tests and are the probable reason for high data scattering.

In general, the inclusion of a finer metal fuel causes a variation of the final agglomerate size. The CCP from P-μAl30 presents a D_{43} of 72.2 µm for the combustion condition of 40 bar. For the same pressure, the P-nAl100L produces CCP having an average size of 22.8 µm. The other two propellants are in the middle of these extreme values. The same data set shows also an unexpected behavior, if pressure dependence is considered. The propellant containing the μAl30 aluminum shows a decrement of the mean agglomerate mass, as the pressure is incremented. This behavior is in line with expectations from the literature and from the modeling, as the rise of pressure causes faster burning rate and lower residence time for agglomerates.[35] On the contrary, the other propellants containing finer metal fuels behave in an opposite manner, incrementing the size of the agglomerates. In the cases of P-nAl800 and P-μAl05 the difference is sensible, while for the P-nAl100L the variation is not very marked.

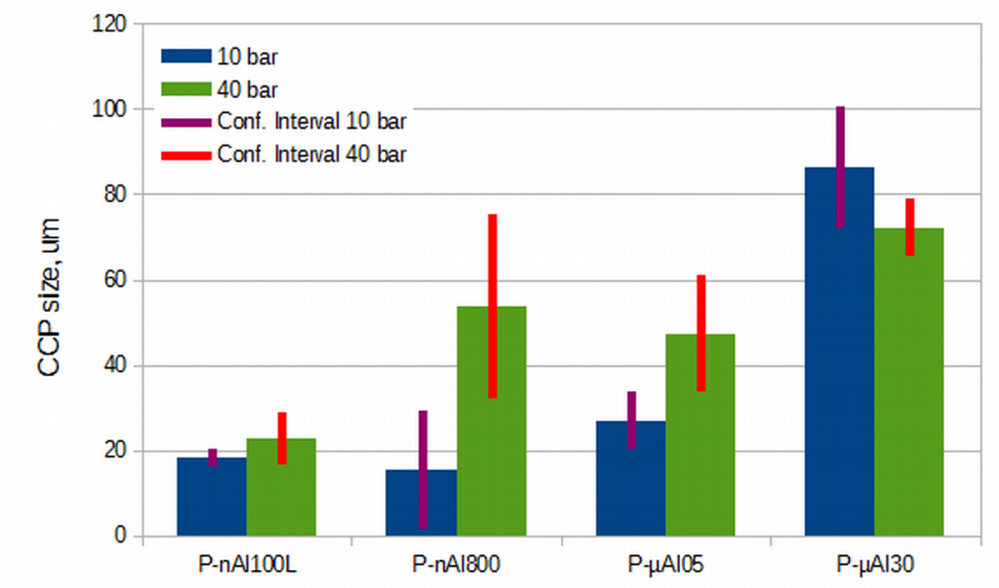

Figure 6. Comparison of CCP size, D_{43}

Figures from 7 to 10 are reporting the detailed particle size distribution curves for the aforementioned conditions. All the distributions feature a bimodal behavior. The coarser mode is located in the range 70 µm to 200 µm and is mainly constituted by the agglomerates. A wide finer mode is also present and spans from about 10 µm down to some hundreds of nanometers. The reader should be aware that 200 nm is the sensitivity limit of the machine used for particle size measurement. It should be also underlined that the D_{43} average tends to over-weight more massive particles. In this case this average diameter is influenced mainly by the coarse mode. For most of the tested propellants, with the exception of P-nAl100L, the increment of the pressure causes a modification of the coarse particle group. In the P-μAl30 the reduction of the particle size at higher pressure is mainly due to a small left shift of the peak, maintaining the same volume fraction. Both P-μAl05 and P-nAl800 increment the size and the mass fraction of the coarse peak at higher pressure. The effect is more evident for P-nAl800 propellant. The behavior of the material containing the nanometric aluminum is different. At higher pressure a third mode having peak at about 60 µm appears, harvesting particles from finer CCP and causing only a minor increment of the D_{43}.

It appears that the different attitudes of agglomeration as a function of pressure are representatives of a variety of mechanisms. On the one side, the residence time criterion may be attributed only to the case where the aluminum is coarse enough (e.g. P-μAl30). In the other tested cases, the trends follow other criteria where original powder reactivity becomes more important. In this respect, the case of P-nAl100L is representative of a condition where the pressure is bringing only small influence on the metal evolution at the burning surface.

V. Conclusion

This paper has presented a systematic and detailed study about some influencing factors on agglomeration. The focus was mainly on powder size and combustion pressure. The experimental data contrasted several propellants featured by the same nominal composition and having aluminum powders ranging from micrometric to nanometric size. The experimental results clearly showed that the introduction of a nanometric metal fuel brings the advantage of smaller agglomerates. The effect of pressure on these materials is not straightforward. Whereas a propellant loaded with a standard micrometric metal fuel reduces the CCP size with the increment of pressure (driven by the residence time), the introduction of a finer metal powder inverts the trend. The behavior is not yet fully assessed but the reactivity of the powder demonstrated to play a fundamental role in the agglomeration regime and in its pressure dependence. In this respect a different attitude towards agglomeration has been identified, when micrometric and nanometric powders are considered. Specifically, the pressure seems to decrease the size of the agglomerate for microaluminum. Such

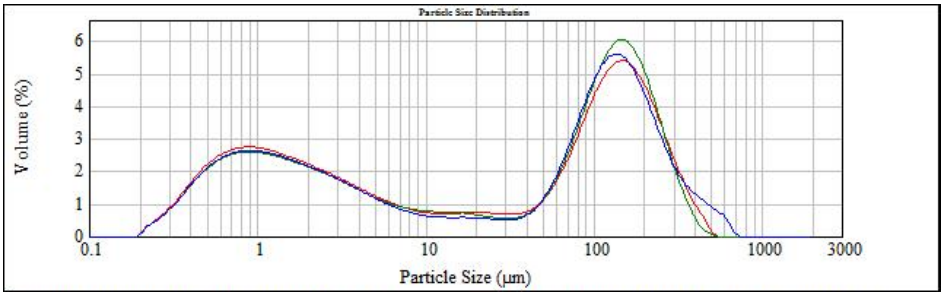

(a) 10 bar

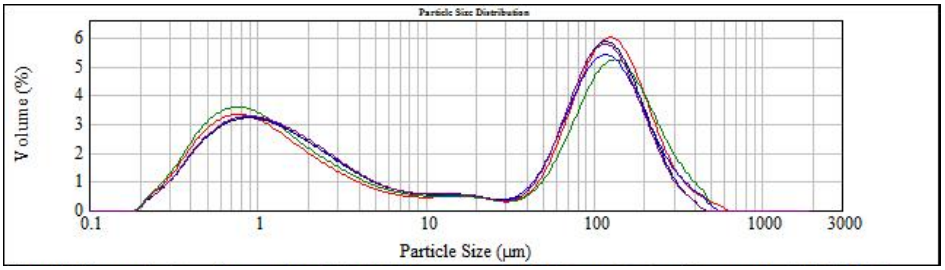

(b) 40 bar

Figure 7. CCP particle size distribution: P-μAl30

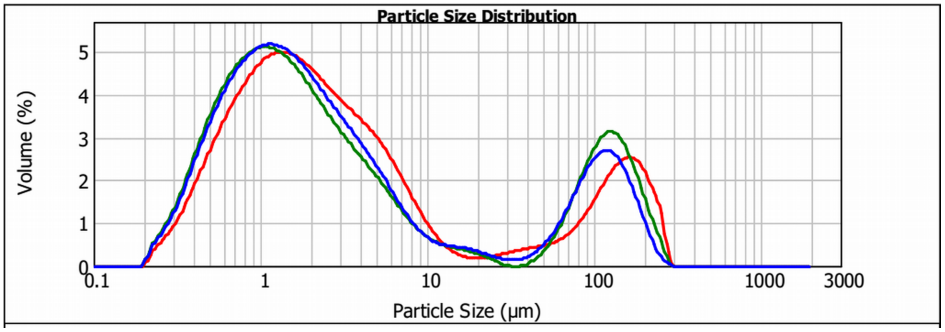

(a) 10 bar

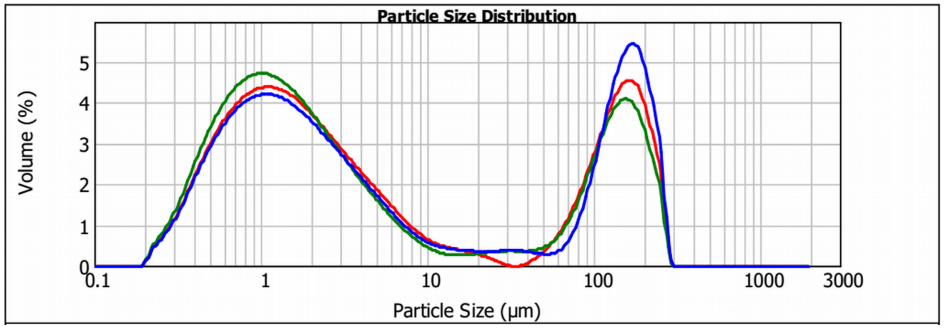

(b) 40 bar

Figure 8. CCP particle size distribution: P-μAl05

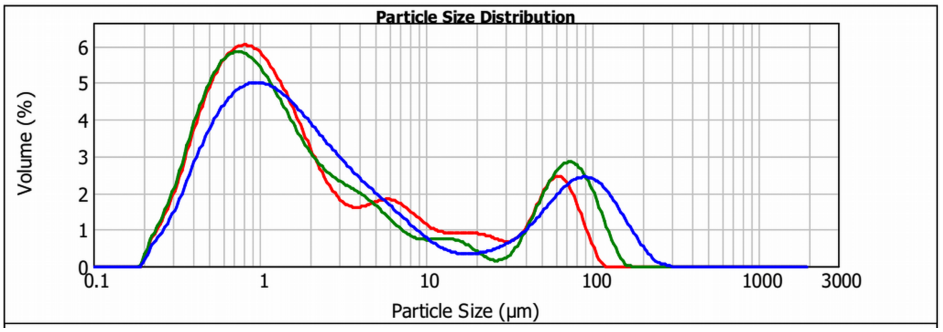

(a) 10 bar

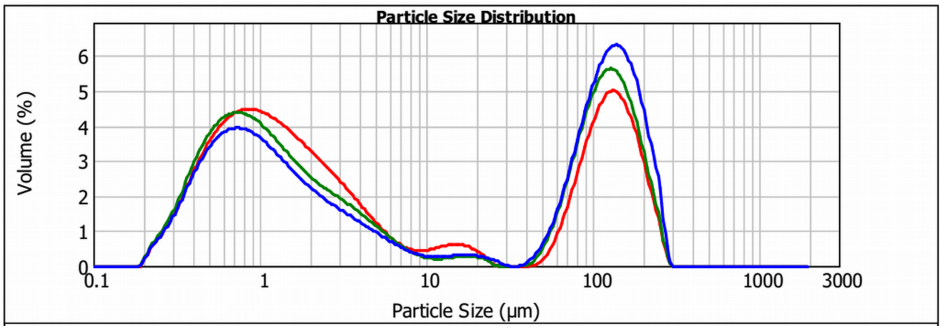

(b) 40 bar

Figure 9. CCP particle size distribution: P-nAl800

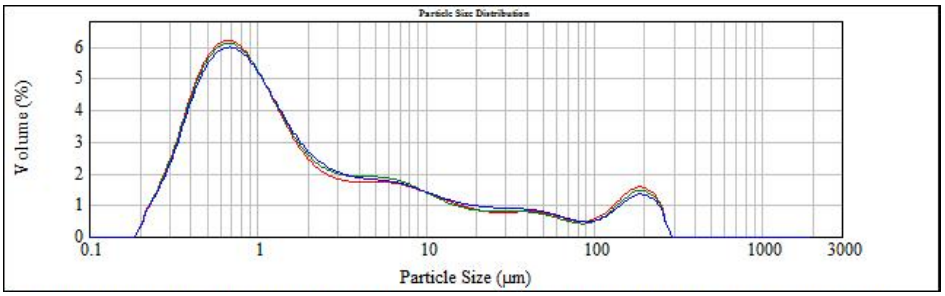

(a) 10 bar

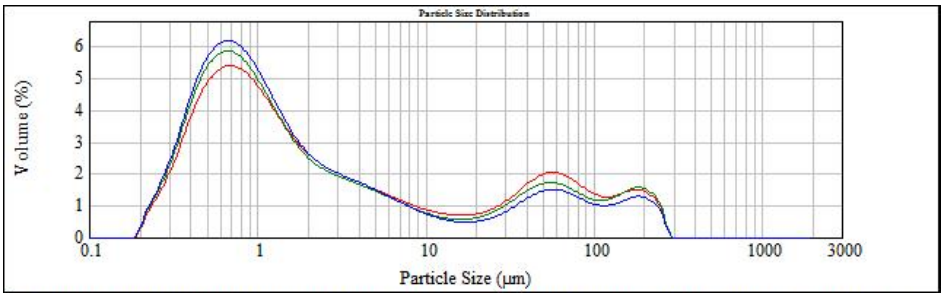

(b) 40 bar

Figure 10. CCP particle size distribution: P-nAl100L

behavior can be connected to the incremented burning rate of the propellant and the reduced residence time of the metal aggregate on the surface. The opposite occurs for nanometric propellants, suggesting a different driver, probably linked to reaction kinetics. Further investigation is still progressing.

The work will extend the propellant database with more metal fuel powders, filling the gaps between the currently tested materials. In addition, a refinement of the collection technique is still on the way, targeting a reduction of the error bars in mean CCP size determination. Finally, the analysis of the residual metal content in collected powders will be included in future investigations.

Acknowledgments

This project has received funding from the European Union's Horizon 2020 research and innovation program under grant agreement no. 638719. The authors wish to thank Mr. Alberto Verga for the support to the DTA/TGA analysis.

References

[1]N. Kubota. *Propellants and Explosives: Thermochemical Aspects of Combustion*. Wiley-VCH, second edition, 2007.

[2]AA.VV. Toxicological profile for aluminum. Technical report, Agency For Toxic Substances And Disease Registry, US Department of Health and Human Services, 2008.

[3]R. W. Hermsen. Aluminum oxide particle size for solid rocket motor performance prediction. *Journal of Spacecraft and Rockets*, 18(6):483–490, 1981.

[4]L. H. Caveny and A. Gany. Breakup of Al/Al_2O_3 agglomerates in accelerating flowfields. *AIAA Journal*, 17(12):1368–1371, Dec 1979.

[5]C. T. Crowe and P. G. Willoughby. A study of particle growth in a rocket nozzle. *AIAA Journal*, 5(7):1300–1304, 1967.

[6]O. G. Glotov, V. V. Karasev, V. E. Zarko, T. D. Fedotova, and M. W. Beckstead. Evolution of aluminum agglomerates moving in combustion products of model solid propellant. *International Journal of Energetic Materials and Chemical Propulsion*, 5(1-6):397–406, 2002.

[7]F. Maggi, S. Dossi, and L. T. DeLuca. Combustion of metal agglomerates in a solid rocket core flow. *Acta Astronautica*, 92(0):163–171, 2012.

[8]F. M. Najjar, J. P. Ferry, A. Haselbacher, and S. Balachandar. Simulations of solid-propellant rockets: Effects of aluminum droplet size distribution. *Journal of Spacecraft and Rockets*, 43(6):1258–1270, 2006.

[9]D. Reydellet. Performance of rocket motors with metallized propellants. Advisory Report AR-230, AGARD, 1986.

[10]AA.VV. Solid rocket motor performance analysis and prediction. Technical Report SP-8039, NASA, May 1971.

[11]L. A. Povinelli. Effect of oxidizer particle size on additive agglomeration. Technical Note D-1438, NASA, November 1962.

[12]V. A. Babuk, V. A. Vasilyev, and M. S. Malakhov. Condensed combustion products at the burning surface of aluminized solid propellant. 15(6):783–793, 1999.

[13]F. Maggi, A. Bandera, L. T. De Luca, V. Thoorens, J. F. Trubert, and T. L. Jackson. Agglomeration in solid rocket propellants: Novel experimental and modeling methods. In *Progress in Propulsion Physics*, volume 2, pages 81–98. EDP Sciences, 2011.

[14]F. Maggi, L. T. DeLuca, and A. Bandera. Pocket model for aluminum agglomeration based on propellant microstructure. *AIAA Journal*, 53(11):3395–3403, 2015.

[15]C. Paravan, F. Maggi, S. Dossi, G. Marra, G. Colombo, and L. Galfetti. Pre-burning characterization of nanosized aluminum in condensed energetic systems. In *Energetic Nanomaterials*, pages 341–368. Elsevier BV, 2016.

[16]J. A. Steinz, P. L. Stang, and M. Summerfield. The burning mechanism of ammonium perchlorate-based composite solid propellants. Technical Report 830, Princeton University, Department of Aerospace and Mechanical Sciences, 1969.

[17]A. P. Il'in, A. A. Gromov, and G. V. Yablunovskii. Reactivity of aluminum powders. *Combustion, Explosion, and Shock Waves*, 37(4):418–422, 2001.

[18]L. DeLuca, L. Galfetti, G. Colombo, F. Maggi, A. Bandera, V. A. Babuk, and V. P. Sinditskii. Microstructure effects in aluminized solid rocket propellants. 26(4):724–733, 2010.

[19]G. V. Ivanov and F. Tepper. Activated aluminum as a stored energy source for propellants. *International Journal of Energetic Materials and Chemical Propulsion*, 4(1-6):636–645, 1997.

[20]A. Dokhan, E. W. Price, J. M. Seitzman, and R. K. Sigman. The ignition of ultra-fine aluminum in ammonium perchlorate solid propellant flames. In *39th AIAA/ASME/SAE/ASEE Joint Propulsion Conference and Exhibit*, number 2003-4810, Huntsville, AL, 2003.

[21]V. Babuk, A. Glebov, I. Dolotkazin, A. Conti, L. Galfetti, L.T. DeLuca, and A. Vorozhtsov. Condensed combustion products from burning of nanoaluminum-based propellants: properties and formation mechanism. In *Progress in Propulsion Physics*, volume 1, pages 3–16. EDP Sciences, 2009.

[22]O. G. Glotov, V. E. Zarko, and M. W. Beckstead. Agglomerate and oxide particles generated in combustion of alex containing solid propellants(exploded aluminum). In *Energetic materials- Analysis, diagnostics and testing*, 2000.

[23]E. L. Dreizin. Metal-based reactive nanomaterials. *Progress in Energy and Combustion Science*, 35:141–167, 2009.

[24]R. A. Yetter, G. A. Risha, and S. F. Son. Metal particle combustion and nanotechnology. *Proceedings of the Combustion Institute*, 32:1819–1838, 2009.

[25]L. Galfetti, L. T. DeLuca, F. Severini, G. Colombo, L. Meda, and G. Marra. Pre and post-burning analysis of nano-aluminized solid rocket propellants. *Aerospace Science and Technology*, 11(1):26–32, 2007.

[26]L. Galfetti, L. T. DeLuca, F. Severini, L. Meda, G. Marra, M. Marchetti, M. Regi, and S. Bellucci. Nanoparticles for solid rocket propulsion. *Journal of Physics: Condensed Matter*, 18(33):S1991–S2005, 2006.

[27]L. Galfetti, F. Severini, L. T. DeLuca, G. Marra, L. Meda, and R. Braglia. Ballistics and condensed combustion residues of aluminized solid rocket propellants. In L. T. DeLuca, L. Galfetti, and R. A. Pesce-Rodriguez, editors, *Proceedings of 9-IWCP, International Workshop on Novel Energetic Materials and Applications*, number 18, La Spezia, Italy, 2004.

[28]L. T. DeLuca, L. Galfetti, F. Severini, L. Meda, G. Marra, A. B. Vorozhtsov, V. S. Sedoi, and V. A. Babuk. Burning of nano-aluminized composite rocket propellants. *Combustion, Explosion and Shock Waves*, 41(6):680–692, 2005.

[29]L. T. DeLuca. Burning of aluminized solid rocket propellants: from micrometric to nanometric fuel size. In P. Huang, Y. Huang, and S. Li, editors, *Proceedings of the 2007 International Autumn Seminar on Propellants, Explosives and Pyrotechnics*, volume VII of *Theory and Practice of Energetic Materials*, pages 277–289, 2007. ISBN: 978-7-03-020254-3.

[30]L. T. De Luca, R. Dondé, L. Galfetti, G. Colombo, F. Maggi, L. Meda, G. Marra, A. Bandera, and D. Orsini. Micro and nano-aluminized solid propellants behavior under transient burning conditions. In *57th International Astronautical Conference*, number IAC-06-C4.2.07, pages 1–11, Valencia, Spain, October 2006. IAF.

[31]L. T. DeLuca, F. Maggi, S. Dossi, M. Fassina, C. Paravan, and A. Sossi. Prospects of aluminum modifications as energetic fuels in chemical rocket propulsion. In *Chemical Rocket Propulsion*, pages 191–233. Springer Nature, 2016.

[32]L. T. DeLuca, L. Galfetti, F. Maggi, G. Colombo, C. Paravan, A. Reina, S. Dossi, M. Fassina, and A. Sossi. Characterization and combustion of aluminum nanopowders in energetic systems. In *Metal Nanopowders*, pages 301–410. Wiley-Blackwell, apr 2014.

[33]E. W. Price. Combustion of metallized propellants. In K. K. Kuo and M. Summerfield, editors, *Fundamental of Solid Propellant Combustion*, volume 90 of *Progress in Astronautics and Aeronautics Series*, pages 479–513. AIAA, New York, NY, USA, 1984.

[34]F. Maggi, A. Bandera, L. Galfetti, L. T. DeLuca, and T. L. Jackson. Efficient solid rocket propulsion for access to space. *Acta Astronautica*, 66(11-12):1563–1573, 2010.

[35]A. Bandera, F. Maggi, and L. T. DeLuca. Agglomeration of aluminized solid rocket propellants. In *45th AIAA/ASME/SAE/ASEE Joint Propulsion Conference and Exhibit*, AIAA Paper 2009-5439, Denver, Colorado, USA, 2009.

[36]P. F. Pokhil, A. F. Belyaev, Yu. V. Frolov, V.S. Logachev, and A.I. Korotkov. Combustion of metal powders in active media. Technical Report AD0769576, Defense Technical Information Center, 1972.

[37]S. Dossi, A. Reina, F. Maggi, and L.T. De Luca. Innovative metal fuels for solid rocket propulsion. *International Journal of Energetic Materials and Chemical Propulsion*, 11(4):299–322, 2012.

[38]Y. Huang, G. A. Risha, V. Yang, and R. A. Yetter. Combustion of bimodal nano/micron-sized aluminum particle dust in air. *Proceedings of the Combustion Institute*, 31:2001–2009, 2007.

[39]S. Brunauer, P. H. Emmett, and E. Teller. Adsorption of gases in multimolecular layers. *Journal of the American Chemical Society*, 60(2):309–319, 1938.

[40]L. Chen, W. Song, J. Lv, X. Chen, and C. Xie. Research on the methods to determine metallic aluminum content in aluminum nanoparticles. *Materials Chemistry and Physics*, 120(2):670–675, 2010.